Proposal of Extended Boundary Integral Equation Method for Rupture Dynamics Interacting With Medium Interfaces

Nobuki Kame[1]
e-mail: kame@eri.u-tokyo.ac.jp

Tetsuya Kusakabe

Earthquake Research Institute,
The University of Tokyo,
Tokyo, Japan 113-0032

The boundary integral equation method (BIEM) has been applied to the analysis of rupture propagation of nonplanar faults in an unbounded homogeneous elastic medium. Here, we propose an extended BIEM (XBIEM) that is applicable in an inhomogeneous bounded medium consisting of homogeneous sub-regions. In the formulation of the XBIEM, the interfaces of the sub-regions are regarded as extended boundaries upon which boundary integral equations are additionally derived. This has been originally known as a multiregion approach in the analysis of seismic wave propagation in the frequency domain and it is employed here for rupture dynamics interacting with medium interfaces in time domain. All of the boundary integral equations are fully coupled by imposing boundary conditions on the extended boundaries and then numerically solved after spatiotemporal discretization. This paper gives the explicit expressions of discretized stress kernels for anti-plane nonplanar problems and the numerical method for the implementation of the XBIEM, which are validated in two representative planar fault problems. [DOI: 10.1115/1.4005899]

1 Introduction

In the field of seismology, earthquake rupture propagation has been modeled as shear crack growth in an elastic medium. Analytic approaches have been limited to simple cases [1] and various numerical techniques have been adopted, such as the finite difference method (FDM) [2], the finite element method (FEM) [3], and the boundary integral equation method (BIEM) [4–9] to seismological applications. Among them, the BIEM is one of the most powerful and accurate numerical methods, especially when the medium can be considered homogeneous. It has been extensively applied to compute the dynamic rupture of nonplanar faults [10–16] because of its built-in advantages. First, the computations are done only on the boundary (i.e., the crack surface), so that geometrical complexities can be introduced rather easily by discretizing the boundary into small finite elements. This further enables us to investigate self-chosen crack paths in a mesh-free manner because crack growth is easily represented by putting an additional boundary element at the crack tip [17]. Second, the elasto-dynamic equation of motion is directly solved to fit the boundary conditions using the theoretical Green's functions, so that a frictional constitutive law can be rigorously introduced on the fault surface. This is an essential part for the analysis of earthquake rupture where a fault friction plays an important role. Robust algorithms have been developed in the past decade, following analytical developments that led to relatively simple and efficient numerical codes to solve nonplanar crack problems, as summarized by Tada [18].

The BIEM has primarily been developed to analyze earthquake rupture in an unbounded homogeneous medium, although recent works succeeded in homogeneous half-space modeling [19,20]. The homogeneous full-space modeling works well for rather deep buried fault earthquakes, but it will lose the validity for shallow earthquakes that would closely approach the ground surface or sediment layers under the ground. In such cases, the stress concentration will be directly affected by their interfaces, and also indirectly by the reflected seismic waves. Such interactions have been mainly investigated by the FEM and the FDM in which medium inhomogeneity can be easily introduced by each element or grid, and significant effects have been found, such as arresting of quasi-static crack growth due to a compliant sediment layer [21] and amplification of strong ground motion in the hanging wall of a dipping fault [22]. Rupture geometry has, however, been mostly modeled as planar because of the difficulty of a mesh arrangement dealing with a complex fault shape, and arbitrary nonplanar geometry thus remains unmodeled.

In this paper we propose an extended BIEM (XBIEM) that can, in principle, deal with the arbitrary geometry of crack growth interacting with medium interfaces. The key idea of the XBIEM is the decomposition of an inhomogeneous medium into homogeneous sub-regions (Fig. 1). We regard the interfaces of subregions as 'extended' boundaries on which the boundary integral equations are additionally derived. This is a multiregion approach widely used in the analysis of seismic wave propagation in the frequency domain [23] and it is employed here for the crack growth problems in the time-domain.

We first formulate the XBIEM, considering a crack in one of the sub-regions and derive the boundary integral equations both on the crack surface and the medium interfaces. All of the boundary integral equations are fully coupled by imposing boundary conditions on the interfaces. In order to solve the coupled equations in the XBIEM, we then develop numerical methods. By applying the collocation method employed with piece-wise constant approximation for the source functions, we derive the discretized stress kernel expressions for anti-plane crack analysis. Our XBIEM is implemented by an explicit time marching scheme by effectively using the discretized kernels. Finally, our XBIEM is tested and validated in two representative planar fault problems with a planar interface.

2 Extended Boundary Integral Equation Method

2.1 Brief Overview of BIEM. We briefly overview the original BIEM for nonplanar rupture analysis in an unbounded
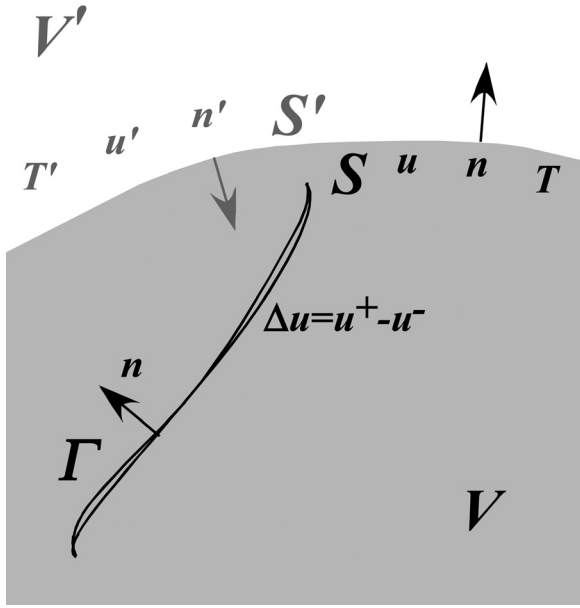

Fig. 1 Schematic illustration of the configuration of a crack and homogeneous sub-regions. A crack surface Γ is in a homogeneous volume V that is bounded by a medium surface S. Another volume V' with a surface S' is adjoining. The two surfaces S and S' are identical except that their normal vectors n and n' are in the opposite direction.

homogeneous medium, as summarized by Tada [18]. It is based on the representation theorem (e.g., Eq. (3.2) in Aki and Richards [24])

$$u_k(\mathbf{x}, t) = \int_\Gamma d\Gamma(\xi) \int_0^t d\tau \, \Delta u_i(\xi, \tau) c_{ijpq} n_j(\xi) \frac{\partial}{\partial \xi_q} G_{kp}(\mathbf{x}, t - \tau; \xi, 0)$$

$$(1)$$

where $u_k(\mathbf{x}, t)$ is the displacement in the kth direction at receiver location $\mathbf{x}$ and time t, Γ is the fault surface, ξ is the source position lying on Γ, $\Delta u_i(\xi, \tau)$ is the slip across Γ in the ith direction at location ξ and time τ, $G_{kp}(\mathbf{x}, t - \tau; \xi, 0)$ is the displacement Green's function denoting the displacement in the kth direction at receiver location $\mathbf{x}$ and time $t - \tau$ due to a unit force in the pth direction applied at source position ξ and time 0, c_{ijpq} is the component of the modulus tensor, and $\mathbf{n}(\xi)$ is the unit normal vector to the fault surface Γ pointing from the negative side Γ^- to the positive side Γ^+ by which $\Delta u_i = u_i^+ - u_i^-$ is defined. The summation over repeated indices is implied, and no body force is assumed in the medium. By combining with Hooke's law, the stress component $\sigma_{kl}(\mathbf{x}, t)$ at any location $\mathbf{x}$ and time t is also represented in terms of the slip on the fault

$$\sigma_{kl}(\mathbf{x}, t) = \sigma_{kl}^0(\mathbf{x}) + \sigma_{kl}^{\Delta u}(\mathbf{x}, t) \tag{2}$$

$$\sigma_{kl}^{\Delta u}(\mathbf{x}, t) = c_{klrs} \frac{\partial}{\partial x_s} u_r(\mathbf{x}, t) = -\int_\Gamma d\Gamma(\xi)$$
$$\times \int_0^t d\tau \, \Delta u_i(\xi, \tau) c_{ijpq} c_{klrs} n_j(\xi) \frac{\partial^2}{\partial x_q \partial x_s} G_{rp}(\mathbf{x}, t - \tau; \xi, 0)$$

$$(3)$$

where $\sigma_{kl}^0(\mathbf{x})$ accounts for an initial field of applied stress that may be present, $\sigma_{kl}^{\Delta u}(\mathbf{x}, t)$ is the incremental stress induced by the slip on the fault (crack), and the reciprocity property for the derivative of the Green's function $\partial G/\partial \xi_q = -\partial G/\partial x_q$ is used.

Equation (3) should hold in the limiting case where the receiver location $\mathbf{x}$ approaches the fault surface Γ. The shear traction $T(\mathbf{x}, t)$

on Γ, that is, the stress component that acts on the fault surface in the direction of a unit vector $\mathbf{t}(\mathbf{x})$ that is tangential to the fault at location $\mathbf{x}$, is therefore given by

$$T(\mathbf{x}, t) = n_k(\mathbf{x}) t_l(\mathbf{x}) \sigma_{kl}(\mathbf{x}, t) = T^0(\mathbf{x}) + T^{\Delta u}(\mathbf{x}, t)$$

$$= T^0(\mathbf{x}) - \int_\Gamma d\Gamma(\xi) \int_0^t d\tau \Delta u_i(\xi, \tau) c_{ijpq} c_{klrs} n_k(\mathbf{x}) t_l(\mathbf{x}) n_j(\xi)$$

$$\times \frac{\partial^2}{\partial x_q \partial x_s} G_{rp}(\mathbf{x}, t - \tau; \xi, 0) \quad (\mathbf{x}, \xi \in \Gamma) \tag{4}$$

where $T^0(\mathbf{x}) = n_k(\mathbf{x}) t_l(\mathbf{x}) \sigma_{kl}^0(\mathbf{x})$ accounts for the initial traction arising from the presence of the initial applied stress and $T^{\Delta u}(\mathbf{x}, t)$ is the incremental traction induced by the slip on the fault. This is the boundary integral equation, which is the fundamental relationship between the spatiotemporal distributions of traction and of slip on the fault embedded in an unbounded homogeneous medium.

2.2 XBIEM Formulation: Multiregion Approach. In the formulation of the XBIEM, we consider an inhomogeneous medium consisting of two homogeneous sub-regions V and V' that are bounded by S and S', respectively (Fig. 1). In order to introduce a medium boundary S into the original BIEM, we shall go back to the representation theorem (e.g., Eqs. (3.1) and (3.2) in Aki and Richards [24])

$$u_k(\mathbf{x}, t) = \int_\Gamma d\Gamma(\xi) \int_0^t d\tau \, \Delta u_i(\xi, \tau) c_{ijpq} n_j(\xi) \frac{\partial}{\partial \xi_q} G_{kp}(\mathbf{x}, t - \tau; \xi, 0)$$

$$+ \int_S dS(\boldsymbol{\eta}) \int_0^t d\tau \left[T_p(\boldsymbol{\eta}, \tau) G_{kp}(\mathbf{x}, t - \tau; \boldsymbol{\eta}, 0) \right.$$

$$\left. - u_i(\boldsymbol{\eta}, \tau) c_{ijpq} n_j(\boldsymbol{\eta}) \frac{\partial}{\partial \eta_q} G_{kp}(\mathbf{x}, t - \tau; \boldsymbol{\eta}, 0) \right] \tag{5}$$

where S is the medium surface, $\boldsymbol{\eta}$ is the location on S, $T_p(\boldsymbol{\eta}, \tau)$ is the pth component of traction on S at location $\boldsymbol{\eta}$ and time τ, $u_i(\boldsymbol{\eta}, \tau)$ is the ith component of displacement on S at time τ, and $\mathbf{n}(\boldsymbol{\eta})$ is a unit normal vector for the surface S pointing outward. Variables regarding the fault surface are taken the same as in the BIEM.

In the original BIEM, the integral on the medium surface S has been omitted. This is justified when S goes to infinity because the integral becomes zero. On the contrary, we have to exactly include the integral on S in the formulation of the XBIEM: the medium surfaces are regarded as the 'extended' boundaries on which boundary integral equations are additionally derived.

It is worth mentioning that the BIEM has also been applied to the field of seismic wave propagation in an inhomogeneous medium consisting of homogeneous sub-regions. The crack surface has been a side issue and usually omitted for mathematical simplicity. Contrary to the crack growth analysis, the medium interface is a 'primary' boundary in this case, and the wave field in each subregion is connected with one another at the interface. Connecting the elastic fields via the interface has been known as a multiregion approach in the BIEM and is mostly applied in the frequency-domain for cases where the interface extent S does not change with time [23]. Here, we apply this approach in the time-domain because the boundary extent may evolve with time.

The stress component σ_{kl} at any location $\mathbf{x}$ and time t is then represented as

$$\sigma_{kl}(\mathbf{x}, t) = \sigma_{kl}^0(\mathbf{x}) + c_{klrs} \frac{\partial}{\partial x_s} u_r(\mathbf{x}, t)$$

$$= \sigma_{kl}^0(\mathbf{x}) + \sigma_{kl}^{\Delta u}(\mathbf{x}, t) + \sigma_{kl}^T(\mathbf{x}, t) + \sigma_{kl}^u(\mathbf{x}, t) \tag{6}$$

where $\sigma_{kl}^T(\mathbf{x}, t)$ and $\sigma_{kl}^u(\mathbf{x}, t)$ are the stresses arising from the distribution of traction and displacement on the medium surface S

$$\sigma_{kl}^T(\mathbf{x},\, t) = \int_S dS(\boldsymbol{\eta}) \int_0^t d\tau\, T_p(\boldsymbol{\eta},\, \tau) c_{klrs} \frac{\partial}{\partial x_s} G_{rp}(\mathbf{x},\, t-\tau;\, \boldsymbol{\eta},\, 0) \quad (7)$$

$$\sigma_{kl}^u(\mathbf{x},\, t) = \int_S dS(\boldsymbol{\eta}) \int_0^t d\tau\, u_i(\boldsymbol{\eta},\, \tau) c_{ijpq} c_{klrs} n_j(\boldsymbol{\eta})$$
$$\times \frac{\partial^2}{\partial x_q \partial x_s} G_{rp}(\mathbf{x},\, t-\tau;\, \boldsymbol{\eta},\, 0) \quad (8)$$

where the property $\partial G/\partial \eta_q = -\partial G/\partial x_q$ is used again.

In this multiregion approach, the boundary integral equations are derived on the medium surfaces and on the fault surface. First, we derive the boundary integral equation on the fault. When $\mathbf{x} \to \Gamma$, the shear traction $T(\mathbf{x},\, t)$ in the direction of $\mathbf{t}(\mathbf{x})$ is given by

$$T(\mathbf{x},\, t) = n_k(\mathbf{x}) t_l(\mathbf{x}) \sigma_{kl}(\mathbf{x},\, t) = T^0(\mathbf{x}) + T^{\Delta u}(\mathbf{x},\, t) + T^T(\mathbf{x},\, t)$$
$$+ T^u(\mathbf{x},\, t) = T^0(\mathbf{x}) + T^T(\mathbf{x},\, t) + T^u(\mathbf{x},\, t)$$
$$- \int_\Gamma d\Gamma(\boldsymbol{\xi}) \int_0^t d\tau\, \Delta u_i(\boldsymbol{\xi},\, \tau) c_{ijpq} c_{klrs} n_k(\mathbf{x}) t_l(\mathbf{x}) n_j(\boldsymbol{\xi})$$
$$\times \frac{\partial^2}{\partial x_q \partial x_s} G_{rp}(\mathbf{x},\, t-\tau;\, \boldsymbol{\xi},\, 0) \quad (\mathbf{x},\, \boldsymbol{\xi} \in \Gamma) \quad (9)$$

where $T^T(\mathbf{x},\, t) = n_k(\mathbf{x}) t_l(\mathbf{x}) \sigma_{kl}^T(\mathbf{x},\, t)$ and $T^u(\mathbf{x},\, t) = n_k(\mathbf{x}) t_l(\mathbf{x}) \sigma_{kl}^u(\mathbf{x},\, t)$ are the incremental tractions observed at $\mathbf{x}$ arising from the traction and displacement sources distributed on the medium surface $\boldsymbol{\eta}(\in S)$. The original boundary integral equation (Eq. (4)) is just modified with these two terms.

The boundary condition on the fault surface is given by an appropriate frictional constitutive law. An example of this is that the shear traction is described in terms of the slip or the slip rate as

$$T(\mathbf{x},\, t) = F(\Delta u,\, \Delta \dot{u}) \quad (\mathbf{x} \in \Gamma(t)) \quad (10)$$

where $\Gamma(t)$ denotes the slipping part of the fault Γ at time t (The geometry of $\Gamma(t)$ may evolve with t, that is, the rupture may grow with time). In earthquake simulations the experimentally derived rate and state-dependent friction has been widely employed as a reasonable constitutive law [25]. It is described by the slip rate $\Delta \dot{u}$ and a general state variable θ which could be the slip on the fault.

When $\mathbf{x} \to S$, the situation becomes slightly different. Equation (7), the surface traction integral term, has to be evaluated at $(\boldsymbol{\eta},\, \tau) = (\mathbf{x},\, t)$ where $T(\mathbf{x},\, t)$ appears in the integrand. The shear traction is thus composed of

$$T(\mathbf{x},\, t) = n_k(\mathbf{x}) t_l(\mathbf{x}) \sigma_{kl}(\mathbf{x},\, t)$$
$$= T^0(\mathbf{x}) + T^{\Delta u}(\mathbf{x},\, t) + T^T(\mathbf{x},\, t)|_{(\boldsymbol{\eta},\, \tau) = (\mathbf{x},\, t)}$$
$$+ T^T(\mathbf{x},\, t)|_{(\boldsymbol{\eta},\, \tau) \neq (\mathbf{x},\, t)} + T^u(\mathbf{x},\, t) \quad (11)$$

With a mathematical property of the Green's function, the integral $T^T(\mathbf{x},\, t)|_{(\boldsymbol{\eta},\, \tau) = (\mathbf{x},\, t)}$ is proven to be equal to $T(\mathbf{x},\, t)/2$ on the condition that S is smooth enough [23]. By canceling the term on both sides, the boundary integral equation on the medium surface is finally given by

$$T(\mathbf{x},\, t)/2 = n_k(\mathbf{x}) t_l(\mathbf{x}) \sigma_{kl}(\mathbf{x},\, t) = T^0(\mathbf{x}) + T^{\Delta u}(\mathbf{x},\, t)$$
$$+ T^T(\mathbf{x},\, t)|_{(\boldsymbol{\eta},\, \tau) \neq (\mathbf{x},\, t)} + T^u(\mathbf{x},\, t) = T^0(\mathbf{x}) + T^{\Delta u}(\mathbf{x},\, t)$$
$$+ \int_S dS(\boldsymbol{\eta}) \int_0^t d\tau\, T_p(\boldsymbol{\eta},\, \tau) c_{klrs} n_k(\mathbf{x}) t_l(\mathbf{x})$$
$$\times \frac{\partial}{\partial x_s} G_{rp}(\mathbf{x},\, t-\tau;\, \boldsymbol{\eta},\, 0)|_{(\boldsymbol{\eta},\, \tau) \neq (\mathbf{x},\, t)}$$
$$+ \int_S dS(\boldsymbol{\eta}) \int_0^t d\tau\, u_i(\boldsymbol{\eta},\, \tau) c_{ijpq} c_{klrs} n_k(\mathbf{x}) t_l(\mathbf{x}) n_j(\boldsymbol{\eta})$$
$$\times \frac{\partial^2}{\partial x_q \partial x_s} G_{rp}(\mathbf{x},\, t-\tau;\, \boldsymbol{\eta},\, 0) \quad (\mathbf{x},\, \boldsymbol{\eta} \in S) \quad (12)$$

where $T^{\Delta u}(\mathbf{x},\, t) = n_k(\mathbf{x}) t_l(\mathbf{x}) \sigma_{kl}^{\Delta u}(\mathbf{x},\, t)$ is the incremental traction observed at $\mathbf{x}$ arising from the slip source distributed on the fault surface $\boldsymbol{\xi}(\in \Gamma)$. Note that the traction at the receiver location $T(\mathbf{x},\, t)$ is represented by the surface traction distribution, excluding the receiver point $T(\mathbf{x},\, t)$, and this enables us to solve the boundary integral equation rather easily in numerical computations.

We then turn to the volume V' where no crack exists. The variables are denoted with a superscript prime when necessary. On the surface S', we derive the boundary integral equation just by omitting $T'^{\Delta u}(\mathbf{x},\, t)$

$$T'(\mathbf{x},\, t)/2 = T'^0(\mathbf{x}) + T'^{T'}(\mathbf{x},\, t)|_{(\boldsymbol{\eta},\, \tau) \neq (\mathbf{x},\, t)} + T'^{u'}(\mathbf{x},\, t) \quad (\mathbf{x},\, \boldsymbol{\eta} \in S') \quad (13)$$

The volumes V and V' are coupled by imposing an appropriate boundary condition on the interface S ($=S'$) based on the contact state. One typical example is that the two surfaces are welded and the traction and displacement are thus continuous on S. The boundary conditions are

$$T(\mathbf{x},\, t) = -T'(\mathbf{x},\, t)$$
$$u(\mathbf{x},\, t) = u'(\mathbf{x},\, t) \quad (\mathbf{x} \in S) \quad (14)$$

Another example is a slipping interface. The traction is again continuous, but the displacement is discontinuous (i.e., the slip $\Delta u = u - u'$ occurs). If the slip is controlled by an appropriate frictional constitutive law $T = f(\Delta u,\, \Delta \dot{u})$, the boundary conditions are given by

$$T(\mathbf{x},\, t) = -T'(\mathbf{x},\, t) = f(\Delta u,\, \Delta \dot{u})$$
$$u(\mathbf{x},\, t) - u'(\mathbf{x},\, t) = \Delta u \quad (\mathbf{x} \in S) \quad (15)$$

where f is a function that differs from one friction law to another.

Finally, we have three boundary integral equations (Eqs. (9), (12), and (13)) and three boundary conditions (Eqs. (10), and (14), or (15)) in terms of the six unknown functions $T(\mathbf{x},\, t)$ and $\Delta u(\mathbf{x},\, t)$ on Γ, $T(\mathbf{x},\, t)$ and $u(\mathbf{x},\, t)$ on S, and $T'(\mathbf{x},\, t)$ and $u'(\mathbf{x},\, t)$ on S', with an appropriate initial condition (e.g., the medium is at rest at $t = 0$). We numerically solve the six coupled equations and obtain the spatiotemporal histories of these six unknown functions, as we will show in the following subsection.

2.3 XBIEM Numerical Method: Anti-Plane Case. In the original BIEM, robust algorithms have been developed in the past decade, following analytical developments that led to relatively simple and efficient numerical codes to solve nonplanar crack problems [18]. Based on these algorithms, here we develop the numerical methods of the XBIEM for solving the coupled boundary integral equations in the anti-plane problems. Some additional steps in the time marching scheme are newly required on the medium surface, whereas the crack part is almost the same as in the original BIEM.

We consider anti-plane crack problems and choose the coordinate axes $(x_1,\, x_2)$ so that the elastic field variables are independent of the third coordinate x_3. Then $\mathbf{x} = (x_1,\, x_2)$ and the relevant boundary variables are $T(\mathbf{x},\, t)$ and $\Delta u_3(\mathbf{x},\, t)$ on Γ, $T(\mathbf{x},\, t)$ and $u_3(\mathbf{x},\, t)$ on S, and $T'(\mathbf{x},\, t)$ and $u_3'(\mathbf{x},\, t)$ on S'. In the anti-plane problems, the shear tractions $T(\mathbf{x},\, t)$ and $T'(\mathbf{x},\, t)$ are in the direction of $\mathbf{t} = (0,0,1)$ and they coincide with the traction vector components $T_3(\mathbf{x},\, t)$ and $T_3'(\mathbf{x},\, t)$.

We first summarize the BIEM numerical methods. The collocation method has been widely used, combined with what is known as the piecewise-constant approximation for the slip rate source function. The nonplanar fault surface is first divided into finite linear segments by a constant length Δs and the variables, $T(\mathbf{x},\, t)$ and $\Delta u_3(\mathbf{x},\, t)$ in the anti-plane cases, are discretized by an interval Δt on each segment. The (i, k)th element lies in the ith fault segment Γ_i

on the fault $\Gamma(= \ \Sigma\Gamma_i)$ and the kth step in the discretized time series. Then the slip rate source function is assumed spatially and temporally piecewise-constant over the (i,k)th element and denoted as $\Delta\dot{u}_{3\ :\ i,k}$. Note that this discretization itself does not limit the receiver location and time $(\mathbf{x}, t)$, that is, the stress $\sigma_{3\alpha}(\mathbf{x}, t)$ (and the shear traction $T(\mathbf{x}, t)$) can be evaluated at any $(\mathbf{x}, t) = (x_1, x_2, t)$. In order to construct the boundary integral equation, we have to choose the collocation point $(\mathbf{x}^{col}, t^{col}) = (x_1^l, x_2^l, t^n)$ where and when the traction is evaluated on the (l,n)th receiver element. It has conventionally been chosen at the midpoint of the segment, and at a certain time during the nth time step, depending on the problems [8]. The traction at the collocation point is denoted by $T_{l,n}$ and the subscript '3' for the variables is omitted hereafter for brevity.

The boundary integral equation, Eq. (4), on the fault surface is thus discretized into the following algebraic form

$$T_{l,n} - T_l^0 = K_0^{\Delta\dot{u}}\Delta\dot{u}_{l,n} + \sum_i \sum_{k=0}^{n-1} K_{l,i\ :\ n-k}^{\Delta\dot{u}}\Delta\dot{u}_{i,k} \ (= T_{l,n}^{\Delta u}) \quad (16)$$

where $\Delta\dot{u}_{i,k}$ is the piecewise-constant slip rate on the (i,k)th source element, and $K_{l,i;n-k}^{\Delta\dot{u}}$ is the stress kernel representing the incremental traction at the collocation point on the (l,n)th receiver element induced by the slip rate. The stress kernels are represented by using the theoretical anti-plane Green's function characterized by the medium rigidity μ and the shear wave velocity β. The right hand side of Eq. (16) corresponds to $T_{l,n}^{\Delta u}$, that is, the incremental traction arising from the slip history on the fault surface. Here, $T_{l,n}^{\Delta u}$ consists of two terms: the first represents an instantaneous response where $K_0^{\Delta\dot{u}} = -\mu/(2\beta)$ relates the current slip rate $\Delta\dot{u}_{l,n}$ to the current traction $T_{l,n}$, and the second indicates the contribution of the past slip rate $(= T_{l,past}^{\Delta u})$.

One of the most essential developments in the BIEM is a very simple and efficient procedure for the stress kernel calculation for the nonplanar fault. Each kernel $K_{l,i;n-k}^{\Delta\dot{u}}$ can be easily represented by a linear sum of the theoretical stress response of $\sigma_{3\alpha}(x_1, x_2, t)$ to the specific semi-infinite distribution of the slip rate $\Delta\dot{u} = H(t)H(x_1)$ lying on the x_1-axis. This was originally developed by Cochard and Madariaga [5] and extensively investigated for 2-D and 3-D crack problems by Tada [18] (see references therein). The stress kernels in the (global) coordinate of interest are computed in the local coordinate: we first take the local coordinate along a source element (i,k) and calculate the $\Delta\dot{u}_{i,k}$ induced stress $\sigma_{3\alpha:l,n}$ at the collocation point on the receiver (l,n) element in the local coordinate. Second, we calculate the shear traction $T = n_\alpha t_3 \sigma_{3\alpha} = t_3 \ (\sigma_{31}n_1 + \sigma_{32}n_2)$, considering the normal and tangential vectors in the local coordinate, and this is $K_{l,i;n-k}^{\Delta\dot{u}}$ in the global coordinate. The BIEM exactly includes the stress interaction among nonplanar fault elements by using the theoretical Green's functions and it is the reason why the BIEM is one of the most accurate numerical methods for nonplanar rupture dynamics.

The discretized boundary integral equation is solved in the following explicit time marching scheme combined with an appropriate boundary condition on the fault surface. If we consider the simplest case $T_{l,n} = 0$ (free surface), for example, the unknown slip rate $\Delta\dot{u}_{l,n}$ is just given in terms of the past slip rate as

$$\Delta\dot{u}_{l,n} = -(T_l^0 + T_{l,past}^{\Delta u})/K_0^{\Delta\dot{u}} \quad (17)$$

Generally, we can solve the two unknowns, $T_{l,n}$ and $\Delta\dot{u}_{l,n}$, under a frictional constitutive law $T_{l,n} = F(\Delta u_{l,n}, \Delta\dot{u}_{l,n}) = F(\Delta\dot{u}_{l,n}\Delta t + \Delta u_{l,n-1}, \Delta\dot{u}_{l,n})$ by an explicit time stepping scheme.

In the development of the XBIEM numerical methods, we apply the same piecewise-constant approximation to the source variables on the extended boundaries, $T(\mathbf{x}, t)$ and $\dot{u}_3(\mathbf{x}, t)$ on S, and $T'(\mathbf{x}, t)$ and $\dot{u}_3'(\mathbf{x}, t)$ on S'. They are discretized and denoted as $T_{i,k}$ and $\dot{u}_{i,k}$ on S, and $T_{i,k}'$ and $\dot{u}_{i,k}'$ on S'. By choosing the collocation points in the same way, $(\mathbf{x}^{col}, t^{col}) = (x_1^l, x_2^l, t^n)$ for the

traction $T_{l,n}$ on the (l,n)th receiver element, the boundary integral equations on Γ, S, and S' are discretized into the following algebraic element, and the boundary integral equations on Γ, S, and S' are discretized into the following algebraic forms

$$T_{l,n} - T_l^0 = (K_0^{\Delta\dot{u}}\Delta\dot{u}_{l,n} + T_{l,past}^{\Delta u}) + T_{l,past}^T + T_{l,past}^u : \ T_{l,n}, \Delta\dot{u}_{l,n} \ \text{on} \ \Gamma \quad (18)$$

$$T_{l,n}/2 - T_l^0 = T_{l,past}^{\Delta u} + T_{l,past}^T + (K_0^{\dot{u}}\dot{u}_{l,n} + T_{l,past}^u) : \ T_{l,n}, \dot{u}_{l,n} \ \text{on} \ S \quad (19)$$

$$T_{l,n}'/2 - T_l'^0 = \ T_{l,past}'^{T'} + (K_0'^{\dot{u}'}\dot{u}_{l,n}' + T_{l,past}'^{u'}) : \ \ T_{l,n}', \ \dot{u}_{l,n}' \ \text{on} \ S' \quad (20)$$

and

$$T_{l,n}^{\Delta u} = K_0^{\Delta\dot{u}}\Delta\dot{u}_{l,n} + T_{l,past}^{\Delta u} \left(T_{l,past}^{\Delta u} = \sum_i \sum_{k=0}^{n-1} K_{l,i;n-k}^{\Delta\dot{u}}\Delta\dot{u}_{i,k} \right) : \quad (21)$$

$$\Delta\dot{u}_{i,k} \ \text{on} \ \Gamma$$

$$T_{l,n}^T = T_{l,past}^T \left(T_{l,past}^T = \sum_i \sum_{k=0}^{n-1} K_{l,i;n-k}^T T_{i,k} \right) : \quad T_{i,k} \ \text{on} \ S \quad (22)$$

$$T_{l,n}^u = K_0^{\dot{u}}\dot{u}_{l,n} + T_{l,past}^u \left(T_{l,past}^u = \sum_i \sum_{k=0}^{n-1} K_{l,i;n-k}^{\dot{u}}\dot{u}_{i,k} \right) : \quad (23)$$

$$\dot{u}_{i,k} \ \text{on} \ S$$

where $T_{l,n}^T$ and $T_{l,n}^u$ represent the incremental traction at the collocation point arising from the traction $T_{i,k}$ and the displacement rate $\dot{u}_{i,k}$ on the medium surface S. Parallel representations hold for $T_{l,n}'^{T'}$ and $T_{l,n}'^u$, but are omitted for brevity. Here, $T_{l,n}^{\Delta u}$ and $T_{l,n}^u$ consist of the instantaneous and past response terms, and the instantaneous term appears only when the source element of $\Delta\dot{u}_{l,n}$ (or $\dot{u}_{l,n}$) coincides with the receiver element of $T_{l,n}$ in the boundary integral equations. Note that Eq. (22) does not involve the instantaneous response $K_0^T T_{l,n}$ because it has been isolated from the integral prior to the discretization and is already canceled at both sides of the boundary integral equation (Eq. (12)) in the XBIEM formulation. Finally, $T_{l,n}$ on the surface S is related to the displacement rate $\dot{u}_{l,n}$ on S whereas $T_{l,n}$ on the crack Γ is related to the slip rate $\Delta\dot{u}_{l,n}$ on Γ.

In order to calculate the stress kernels in the XBIEM, we employ the same procedure as in the BIEM. We employ the same specific function T, $\dot{u} = H(t)H(x_1)$ distributed on the x_1-axis and derive the theoretical stress response $\sigma_{3\alpha}$ at an arbitrary receiver point (x_1, x_2, t). Note that the stress responses arising from the displacement rate on the surface in Eq. (8) are just the negative of those for the slip rate on the fault in Eq. (3). We can, therefore, make use of the previously derived kernel function for the displacement rate. This immediately leads to the instantaneous response $K_0^{\dot{u}} = -K_0^{\Delta\dot{u}} = \mu/(2\beta)$. The stress responses induced by the traction rate are newly derived and completely described in Appendix A.

The discretized boundary integral equations enable us to solve the six unknowns at the time step n in the following explicit time marching scheme. When we consider the fault surface, $T_{l,n}$ and $\Delta\dot{u}_{l,n}$ on Γ, the integral equation (18) is decoupled from the other two at the current time step, so that we can solve two unknowns, $T_{l,n}$ and $\Delta\dot{u}_{l,n}$, under the boundary condition given on a fault surface. If we simply consider a traction free fault ($T_{l,n} = 0$), the unknown slip rate is determined as

$$\Delta\dot{u}_{l,n} = -(T_l^0 + T_{l,past}^{\Delta u} + T_{l,past}^T + T_{l,past}^u)/K_0^{\Delta\dot{u}} \quad (24)$$

It is almost the same as Eq. (17), except for the two additional traction terms, $T_{l,past}^T$ and $T_{l,past}^u$, arising from the medium surface

S. The two unknowns can be determined in an explicit time stepping if we consider a frictional constitutive law (e.g., $T_{l,n} = F(\Delta u_{l,n}, \Delta \dot{u}_{l,n})$) on the fault.

On the medium interface, we have four equations (two boundary integral equations and two boundary conditions) for four unknowns $T_{l,n}$, $\dot{u}_{l,n}$, $T'_{l,n}$, and $\dot{u}'_{l,n}$. When the two volumes are welded at the interface and the boundary conditions are given by Eqs. (14), the solutions are

$$\dot{u}_{l,n} \, (=\dot{u}'_{l,n}) = -(T^{\Delta u}_{l,past} + T^T_{l,past} + T^u_{l,past} + T'^{T'}_{l,past} + T'^{u'}_{l,past})/$$
$$(K^{\dot{u}}_0 + K'^{\dot{u}'}_0) \tag{25}$$

$$T_{l,n} \, (=-T'_{l,n}) = 2(K^{\dot{u}}_0 \dot{u}_{l,n} + T^0_l + T^{\Delta u}_{l,past} + T^T_{l,past} + T^u_{l,past}) \tag{26}$$

On the contrary, when the interface is slipping, we can also determine the four unknowns in an explicit time scheme. If we consider a traction free interface, for example, the solutions are

$$\dot{u}_{l,n} = -(T^0_l + T^{\Delta u}_{l,past} + T^T_{l,past} + T^u_{l,past})/K^{\dot{u}}_0 \tag{27}$$

$$\dot{u}'_{l,n} = -(T'^0_l + T'^{T'}_{l,past} + T'^{u'}_{l,past})/K'^{\dot{u}'}_0 \tag{28}$$

$$T_{l,n} = T'_{l,n} = 0 \tag{29}$$

If the boundary conditions are given by Eqs. (15), we can also determine the four unknowns.

Last, we consider two typical cases with the Earth's surface where no adjacent volume V' exists. We have two unknowns $T_{l,n}$ and $\dot{u}_{l,n}$ on S. When $T_{l,n}$ is specified (i.e., the Neumann condition), $\dot{u}_{l,n}$ is determined as

$$\dot{u}_{l,n} = -(T^0_l + T^{\Delta u}_{l,past} + T^T_{l,past} + T^u_{l,past} - T_{l,n}/2)/K^{\dot{u}}_0 \tag{30}$$

and when $\dot{u}_{l,n}$ is specified (i.e., the Dirichlet condition), $T_{l,n}$ is determined as

$$T_{l,n} = 2(K^{\dot{u}}_0 \dot{u}_{l,n} + T^0_l + T^{\Delta u}_{l,past} + T^T_{l,past} + T^u_{l,past}) \tag{31}$$

Repeating the preceding time marching scheme step by step, we investigate the time evolution of boundary variables in the XBIEM.

3 XBIEM Validation Tests

We have shown the explicit time marching scheme of the XBIEM for dynamic rupture interacting with medium interfaces. Here, the XBIEM is implemented and validated in two classical planar crack problems for which analytic solutions exist in limited aspects: one is in an unbounded homogeneous medium and another is in a bimaterial.

3.1 Slip-Rate on Instantaneous Crack. Burridge [26] found an analytic solution for the slip rate on a finite anti-plane crack without friction in an unbounded homogeneous medium. The crack lying on the x_1-axis with length $2a$ instantaneously appears along its entire length at $t=0$ with a stress drop $\Delta\sigma$ and does not propagate. As a validation test of our XBIEM, we compare the numerical solution with the analytic one, as was done in the development of the BIEM [5].

In order to compute the full-space problem by using the XBIEM, an equivalent problem is considered in a homogeneous half-space (consider only the upper half-space V^+ bounded by a surface S^+ on the x_1-axis in Fig. 2). The equivalent problem is attained by imposing the stress boundary condition on the crack region ($T=0$ for $-a \leq x_1 \leq a$) and the displacement boundary condition outside it ($u_3 = 0$ for $|x_1| > a$) under a homogeneously applied initial stress $\sigma^0_{32} = \Delta\sigma$. The displacement condition comes from the antisymmetry of the displacement field in the full space
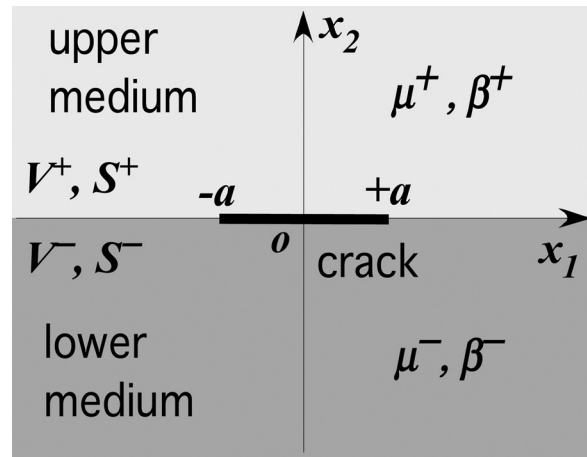

Fig. 2 Configuration of a bimaterial consisting of two homogeneous half-spaces ($x_2 > 0$ for V^+ and $x_2 < 0$ for V^-) bounded by surfaces $S^\pm$ adjoining on the x_1-axis. Each medium is characterized by the rigidity $\mu^\pm$ and the shear wave velocity $\beta^\pm$. In the validation tests shown in Figs. 3 and 4, an initial crack with length $2a$ is assumed on the x_1-axis.

with respect to the x_1-axis. With a sudden stress drop at $t=0$, we investigate the displacement rate on the crack region by using Eq. (30) and the traction evolution outside it by using Eq. (31).

We compare the slip rate as a function of time for the analytical solution and for the numerical one (Fig. 3). We see that the numerical solution is very close to the analytical one, except near the arrival of the stopping phases, indicated by arrows, arising from the edges of the crack. The accuracy of the numerical method is verified in this simple problem.

3.2 Spontaneous Crack Growth Along a Bimaterial Interface. Next, the XBIEM is tested in the simulation of spontaneous growth of a crack along a planar bimaterial interface at which two homogeneous half-spaces $V^\pm$ with surfaces $S^\pm$ are adjoining on the x_1-axis (Fig. 2). Each homogeneous material is characterized by the medium rigidity $\mu^\pm$ and the shear wave velocity $\beta^\pm$, respectively. The analytically derived stress coefficient for a semi-infinite kinematic rupture propagating with a constant
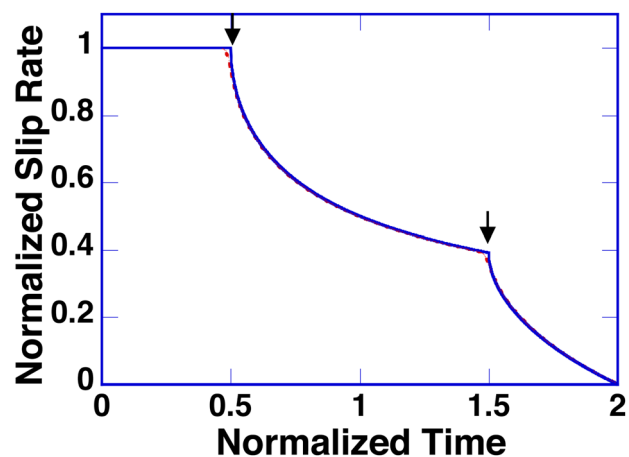

Fig. 3 Analytic (solid line) and numerical solution (dotted line) for the 101th element of an instantaneous crack discretized into 402 elements. The computation is done with normalized quantities: traction $T_{nrml} = T/\Delta\sigma$, length $x_{nrml} = x/a$, time $t_{nrml} = t/(\alpha/\beta)$ and displacement velocity $\dot{u}_{nrml} = \dot{u}/(\beta\Delta\sigma/\mu)$, where $\Delta\sigma$ is the stress drop, a is the crack half-length, μ is the medium rigidity, and β is the shear wave velocity of the medium. A time step is assumed as $\Delta t = \Delta s/(2\beta)$.
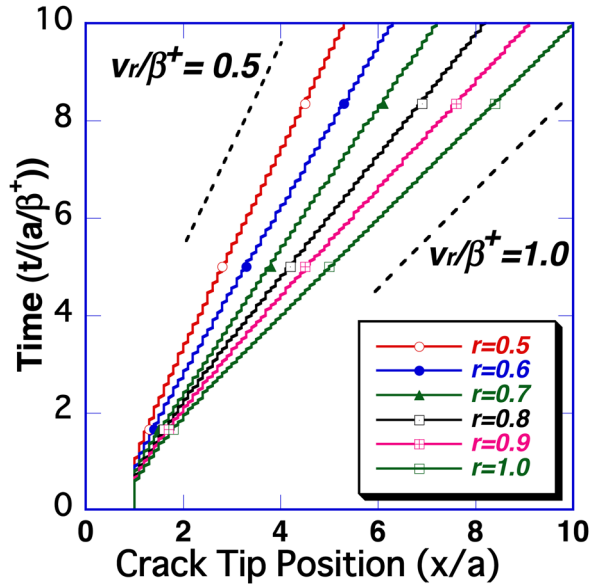
Fig. 4 Spatiotemporal evolution of the crack tip position spontaneously propagating along the bimaterial interface for different material contrasts $r = 0.5$, 0.6, 0.7, 0.8, 0.9, and 1.0. The material contrast is characterized by $r = \beta^-/\beta^+$, the ratio of the lower medium shear wave velocity to the upper velocity. Unit quantities for the computation are based on those in the upper medium. The initial crack with length $2a$ is discretized by 40 elements, and the unit time a/β^+ is discretized by 40 time steps. The interface is represented by 800 elements, which is large enough to eliminate the diffracted wave from the artificial edges of the computational domain coming back to the crack tip. The predicted upper limit rupture velocities for $r = 0.5$ ($v_r/\beta^+ = 0.5$) and $r = 1.0$ ($v_r/\beta^+ = 1.0$) are plotted for reference.

sub-shear rupture velocity $v_r(<\beta^{\pm})$ shows that the stress concentration approaches zero when $v_r \to \beta^-$, where β^- indicates the lower shear wave velocity in the bimaterial (see Appendix B). It implies that the upper limit of the rupture velocity is β^- for spontaneously accelerating crack growth from a static state. This prediction is confirmed by numerical simulations by the XBIEM.

We start the spontaneous rupture from a seed crack with length $2a$ instantaneously appearing at $t = 0$ under a homogeneously applied initial stress $\sigma_{32}^0 = \Delta\sigma$. On the crack surface (= slipping interface), the stress boundary condition is given by $T = 0$ (the stress drop is $\Delta\sigma$). Otherwise, the two volumes are welded at the interface and the boundary conditions are given by Eq. (14). Here, the crack growth is assumed to be described by a finite stress criterion τ_p: if the shear traction T at the crack tip exceeds τ_p, the crack propagates by one element at that time step. We set $\tau_p = 3\Delta\sigma$. By applying the time stepping scheme in Eqs. (27), (28), and (29) to the slipping interface and Eqs. (25) and (26) to the welded interface, we determine the spatiotemporal history of the traction and the displacement rate on both S^+ and S^-.

Figure 4 shows the spatiotemporal evolution of the crack tip position for different material contrast $r = \beta^-/\beta^+$. It clearly shows that the rupture velocity finally approaches the lower shear wave velocity of the bimaterial. The XBIEM for rupture dynamics interacting with medium interface is successfully validated in this problem.

4 Conclusions

Aiming for the simulation of nonplanar earthquake rupture interacting with medium interfaces, we proposed an extended boundary integral equation method (XBIEM). In the formulation of the XBIEM, we employ a multiregion approach where the interfaces of the sub-regions are regarded as extended boundaries on which boundary integral equations are additionally derived.

We derived a complete set of the boundary integral equations that are fully coupled by boundary conditions on the extended boundaries.

We next developed the numerical methods necessary for solving the coupled boundary integral equations for anti-plane problems. Based on the established BIEM algorithms, we derived the discretized stress kernels that represent dynamic interactions among nonplanar boundary elements. We developed an explicit time marching scheme in order to determine the spatiotemporal functions on all of the boundaries, the crack surface, and the medium surfaces.

We tested and validated our XBIEM in two classical problems for which analytic solutions exist. The XBIEM calculation of the slipping rate on a instantaneous crack in an unbounded homogeneous medium showed a good agreement with the analytic solution. We then tested our XBIEM in a bimaterial. In the simulation of spontaneous rupture propagation along a bimaterial interface, the numerical results successfully agreed with the theoretical prediction that the rupture velocity approached the lower shear wave velocity of the bimaterial.

Although we have just demonstrated our XBIEM in the simple planar crack problems with planar surfaces, the XBIEM is, in principle, applicable to the dynamic rupture of nonplanar faults. The kernels derived here are enough for modeling the arbitrary nonplanar geometry of faults, and can be applied to a self-chosen crack path modeling with a mesh-free manner. We challenge it in order to investigate the effects of stress interaction with medium interfaces on the formation of nonplanar geometry of earthquake faults.

Our numerical development was made only in anti-plane cases, although our formulation works in all of the 2-D and 3-D problems. We hope that the XBIEM is applied to various problems in the field of earthquake seismology.

Appendix A: Convolution Coefficients for Elastic Stress Field

Here we give the convolution coefficients for the discrete expressions of the stress field arising from the slip rate $\Delta\dot{u}_3$ on the crack surface Γ, the traction T_3 on the medium surface S, and the displacement rate $\dot{u}_3$ on S

$$
\sigma_{3\alpha}^{\Delta u}(x_1^l, x_2^m, t^n) = -\int_\Gamma d\xi_1 \int_0^t d\tau \, \Delta u_3(\xi_1, \tau) \mu^2 \frac{\partial^2}{\partial x_\alpha \partial x_2} G_{33}
$$
$$
= \sum_{i,k} K_{l,m,n,i,k}^{\sigma_{3\alpha} : \Delta\dot{u}} \Delta\dot{u}_{i,k} \tag{A1}
$$

$$
\sigma_{3\alpha}^{T}(x_1^l, x_2^m, t^n) = +\int_S d\xi_1 \int_0^t d\tau \, T_3(\xi_1, \tau) \mu \frac{\partial}{\partial x_\alpha} G_{33}
$$
$$
= \sum_{i,k} K_{l,m,n,i,k}^{\sigma_{3\alpha} : T} T_{i,k} \tag{A2}
$$

$$
\sigma_{3\alpha}^{u}(x_1^l, x_2^m, t^n) = +\int_S d\xi_1 \int_0^t d\tau u_3(\xi_1, \tau) \mu^2 \frac{\partial^2}{\partial x_\alpha \partial x_2} G_{33}
$$
$$
= \sum_{i,k} K_{l,m,n,i,k}^{\sigma_{3\alpha} : \dot{u}} \dot{u}_{i,k} \tag{A3}
$$

where G_{33} denotes the anti-plane Green's function

$$G_{33}(x_1^l - \xi_1, x_2^m, t^n - \tau; 0, 0, 0) = \frac{1}{2\pi\mu} \frac{H((t^n - \tau) - r/\beta)}{\sqrt{(t^n - \tau)^2 - (r/\beta)^2}}$$

$$r \equiv \sqrt{(x_1^l - \xi_1)^2 + (x_2^m)^2} \qquad (A4)$$

and $H(\cdot)$ is the Heaviside step function. A temporally and spatially piecewise-constant interpolation is applied to the slip rate, traction, and displacement rate (all assumed to distributed on the x_1-axis) as

$$\Delta \dot{u}_3(x_1, t) = \sum_{i,k} \Delta \dot{u}_{i,k} d_{i,k}(x_1, t), \ T_3(x_1, t)$$
$$= \sum_{i,k} T_{i,k} d_{i,k}(x_1, t), \ \dot{u}_3(x_1, t) = \sum_{i,k} \dot{u}_{i,k} d_{i,k}(x_1, t) \quad (A5)$$

$$d_{i,k}(x_1, t) \equiv [H(x_1 - x_1^i + \Delta s/2) - H(x_1 - x_1^i - \Delta s/2)]$$
$$\times [H(t - t_{\text{short}}^k) - H(t - t_{\text{long}}^k)] \qquad (A6)$$

$$t_{\text{short}}^k \equiv t^k - e_t \Delta t, \quad t_{\text{long}}^k \equiv t^k + (1 - e_t)\Delta t, \quad 0 < e_t < 1 \quad (A7)$$

After applying the integration by parts with respect to τ for the reduction of the hyper-singularity that would appear in the second order derivative of the Green's function, we substitute the discretized functions, Eq. (A5), for the integrals and derive the coefficients. The coefficients for the stress are

$$K_{l,m,n,i,k}^{\sigma_{3\alpha}:src} \equiv I^{\sigma_{3\alpha}:src}\left(x_1^l - x_1^i + \frac{1}{2}\Delta s, x_2^m, t^n - t_{\text{short}}^k\right)$$
$$- I^{\sigma_{3\alpha}:src}\left(x_1^l - x_1^i - \frac{1}{2}\Delta s, x_2^m, t^n - t_{\text{short}}^k\right)$$
$$- I^{\sigma_{3\alpha}:src}\left(x_1^l - x_1^i + \frac{1}{2}\Delta s, x_2^m, t^n - t_{\text{long}}^k\right)$$
$$+ I^{\sigma_{3\alpha}:src}\left(x_1^l - x_1^i - \frac{1}{2}\Delta s, x_2^m, t^n - t_{\text{long}}^k\right) \qquad (A8)$$

and

$$I^{\sigma_{31}:\Delta\dot{u}}(\mathbf{x}, t) = -\frac{\mu}{2\beta}\left[-\frac{x_2}{\pi r}H\left(t - \frac{r}{\beta}\right)\sqrt{(\beta t/r)^2 - 1}\right] \qquad (A9)$$

$$I^{\sigma_{32}\Delta\dot{u}}(\mathbf{x}, t) = -\frac{\mu}{2\beta}\left[H(x_1)H\left(t - \frac{|x_2|}{\beta}\right) + \frac{1}{\pi}\text{sgn}(x_1)\right.$$
$$\left. \times H\left(t - \frac{r}{\beta}\right)\left(\frac{|x_1|}{r}\sqrt{(\beta t/r)^2 - 1} - \text{Arccos}\frac{|x_1|}{\beta u_\beta}\right)\right] \qquad (A10)$$

$$I^{\sigma_{31}:T}(\mathbf{x}, t) = -\frac{1}{4\pi}H\left(t - \frac{r}{\beta}\right)\log\frac{t - \sqrt{t^2 - (r/\beta)^2}}{t + \sqrt{t^2 - (r/\beta)^2}} \qquad (A11)$$

$$I^{\sigma_{32}:T}(\mathbf{x}, t) = -\text{sgn}(x_2)H(x_1)H\left(t - \frac{|x_2|}{\beta}\right)\frac{1}{2}$$
$$+ \text{sgn}(x_1)\text{sgn}(x_2)H\left(t - \frac{r}{\beta}\right)\frac{1}{2\pi}\text{Arccos}\frac{|x_1|t}{ru_\beta} \quad (A12)$$

$$I^{\sigma_{31}:\dot{u}}(\mathbf{x}, t) = -I^{\sigma_{31}:\Delta\dot{u}}(\mathbf{x}, t) \qquad (A13)$$

$$I^{\sigma_{32}:\dot{u}}(\mathbf{x}, t) = -I^{\sigma_{32}:\Delta\dot{u}}(\mathbf{x}, t) \qquad (A14)$$

where $u_\beta \equiv \sqrt{t^2 - (x_2/\beta)^2}$. Note that $K_{l,m,n,i,k}^{\sigma_{3\alpha}:\Delta\dot{u}}$ had been derived in Tada and Madariaga [8] and is reproduced here for the reader's convenience.

Appendix B: Shear Stress for Kinematic Rupture at a Bimaterial Interface

We consider a bimaterial in which two isotropic homogeneous elastic half-spaces are adjoining at the x_1-axis. We presume anti-plane deformation in the x_3-direction, and the equations of motion are thus

$$\frac{1}{(\beta^\pm)^2}\frac{\partial^2 u_3^\pm}{\partial t^2} = \frac{\partial^2 u_3^\pm}{\partial x_1^2} + \frac{\partial^2 u_3^\pm}{\partial x_2^2} \qquad (B1)$$

where $u_3^\pm$ are the displacements, $\beta^\pm$ are the shear wave velocities of the half-spaces, and $\pm$ denotes the quantities in the upper $(x_2 > 0)$ and lower $(x_2 < 0)$ half-spaces, respectively. We denote the medium rigidities $\mu^\pm$ and assume $\beta^- \leq \beta^+$.

We consider a kinematic rupture propagating at the bimaterial interface in the $+x_1$ direction with a prescribed rupture velocity and a presumed displacement discontinuity. We shall consider the case in which phenomena appear to be stationary if looked at in a coordinate

$$x_1' = x_1 - v_r t, \ x_2' = x_2, \ t' = t \qquad (B2)$$

on the condition that the rupture is semi-infinite and propagating from $t = -\infty$ with a constant rupture velocity v_r. The boundary condition regarding the displacement discontinuity across the rupture is given by

$$u_3^+(x_1', +0, t') - u_3^-(x_1', -0, t') = \Delta u H(-x_1') \qquad (B3)$$

where Δu is a constant and $H(\cdot)$ is the Heaviside step function. The stress across the interface is continuous, so that the stress boundary condition is given by

$$\mu^+ \frac{\partial u_3^+}{\partial x_2'}(x_1', +0, t') = \mu^- \frac{\partial u_3^-}{\partial x_2'}(x_1', -0, t') \qquad (B4)$$

If looked at in the moving coordinate, Eq. (B1) is rewritten as

$$(\gamma^\pm)^2 \frac{\partial^2 u_3^\pm}{\partial x_1'^2} + \frac{\partial^2 u_3^\pm}{\partial x_2'^2} = 0 \qquad (B5)$$

where $\gamma^\pm = \sqrt{1 - \left(\frac{v_r}{\beta^\pm}\right)^2}$, and v_r is assumed sub-shear velocity (i.e., $v_r \leq \beta^\pm$).

By applying the Fourier transform to $u_3(x_1')$ in Eq. (B5), the solutions $\tilde{u}_3(k_1)$ in the wavenumber domain that are bounded at $x_2' \to \pm\infty$ shall be

$$\tilde{u}_3^\pm(k_1, x_2') = A^\pm \exp(\mp|k_1|\gamma^\pm x_2') \qquad (B6)$$

where $A^\pm$ are constant coefficients that should be constrained by the boundary conditions (Eqs. (B3) and (B4)), and they, therefore, lead to

$$A^\pm = \pm \frac{\mu^\mp \gamma^\mp}{\mu^+ \gamma^+ + \mu^- \gamma^-} \frac{i}{k_1} \qquad (B7)$$

By applying the inverse Fourier transform to $\tilde{u}_3(k_1, x_2')$ with the preceding coefficients, we shall obtain the displacement $u_3(x_1', x_2')$ that satisfies the boundary conditions. Followed by Hooke's law, the shear stress σ_{32} near the propagating rupture front is finally expressed by

$$\sigma_{32}^\pm(x_1', x_2') = \frac{\Delta u}{\pi} \frac{\mu^+ \mu^- \sqrt{1 - \left(\frac{v_r}{\beta^+}\right)^2}\sqrt{1 - \left(\frac{v_r}{\beta^-}\right)^2}}{\mu^+ \sqrt{1 - \left(\frac{v_r}{\beta^+}\right)^2} + \mu^- \sqrt{1 - \left(\frac{v_r}{\beta^-}\right)^2}}$$
$$\times \frac{x_1'}{x_1'^2 + 1 - \left(\frac{v_r}{\beta^\pm}\right)^2 x_2'^2}. \qquad (B8)$$

This indicates that the shear stress concentration becomes zero if the rupture velocity v_r increases to be the lower shear wave velocity β^-. It implies that the upper limit of the rupture velocity in the sub-shear regime would be β^- in the bimaterial.

References

[1] Kostrov, B., 1966, "Unsteady Propagation of Longitudinal Shear Cracks," J. Appl. Math. Mech., **30**, pp. 1241-1248.

[2] Madariaga, R., 1976, "Dynamics of Expanding Circular Fault," Bull. Seismol. Soc. Am., **66**, pp. 639–666.

[3] Oglesby, D. D., Archuleta, R. J., and Nielsen, S. B., 1998, "Earthquakes on Dipping Faults: the Effects of Broken Symmetry," Science, **280**, pp. 1055–1059.

[4] Andrews, D. J., 1976, "Rupture Velocity of Plane Strain Shear Crack," J. Geophys. Res., **81**, pp. 5679–5687.

[5] Cochard, A. and Madariaga, R., 1994, "Dynamic Faulting Under Rate-Dependent Friction," Pure Appl. Geophys., **142**, pp. 419–445.

[6] Kame, N. and Yamashita T., 1997, "Dynamic Nucleation Process of Shallow Earthquake Faulting in a Fault Zone," Geophys. J. Int., **128**, pp. 204–216.

[7] Lapsta, N., Rice, J. R., Ben-Zion, Y., and Zheng, G., 2000, "Elastodynamic Analysis for Slow Tectonic Loading with Spontaneous Rupture Episodes on Faults with Rate- and State-dependent Friction," J. Geophys. Res., **105**, pp. 23765–23790.

[8] Tada, T. and Madariaga, R., 2001, "Dynamic Modelling of the Flat 2-D Crack by a Semi-analytic BIEM Scheme," Int. J. Numer. Mech. Eng., **50**, pp. 227–251.

[9] Kame, N. and Uchida, K., 2008, "Seismic Radiation from Dynamic Coalescence, and the Reconstruction of Dynamic Source Parameters on a Planar Fault," Geophys. J. Int., **174**, pp. 696–706.

[10] Tada, T. and Yamashita T., 1997, "Non-Hypersingular Boundary Integral Equations for Two-Dimensional Non-Planar Crack Analysis," Geophys. J. Int., **130**, pp. 269–282.

[11] Kame, N. and Yamashita T., 1999, "A New Light on Arresting Mechanism of Dynamic Earthquake Faulting," Geophys. Res. Lett., **26**, pp. 1997–2000.

[12] Aochi, H., Fukuyama, E., and Matsu'ura, M., 2000, "Spontaneous Rupture Propagation on a Nonplanar Fault in 3-D Elastic Medium," Pure Appl. Geophys., **157**, pp. 2003–2027.

[13] Kame, N. and Yamashita T., 2003, "Dynamic Branching, Arresting of Rupture and the Seismic Wave Radiation in a Self-Chosen Crack Path Modelling," Geophys. J. Int., **155**, pp. 1042–1050.

[14] Kame, N., Rice, J. R., and Dmowska, R., 2003, "Effects of Prestress State and Rupture Velocity on Dynamic Fault Branching," J. Geophys. Res., **108**(B5), p. 2265.

[15] Bhat, H., Dmowska, R., Rice, J. R., and Kame, N., 2004, "Dynamic Slip Transfer from the Denali to Totschunda Faults, Alaska: Testing Theory for Fault Branching," Bull. Seismol. Soc. Am., **94**, pp. 202–213.

[16] Ando, R., Kame, N., and Yamashita, T., 2007, "An Efficient Boundary Integral Equation Method Applicable to the Analysis of Non-planar Fault Dynamics," Earth Planets Space, **59**, pp. 363–373.

[17] Kame, N. and Yamashita T., 1999, "Simulation of the Spontaneous Growth of a Dynamic Crack without Constraints on the Crack Tip Path," Geophys. J. Int., **139**, pp. 345–358.

[18] Tada, T., 2009, "Boundary Integral Equation Method for Earthquake Rupture Dynamics," *Fault-Zone Properties and Earthquake Rupture Dynamics*, E. Fukuyama,. ed., Elsevier Academic, Burlington, MA, pp. 217–267.

[19] Zhang, H. and Chen, X., 2006, "Dynamic Rupture on a Planar Fault in Three-dimensional Half-space—1. Theory," Geophys. J. Int., **164**, pp. 633–652.

[20] Hok, S. and Fukuyama, E., 2011, "A New BIEM for Rupture Dynamics in Half-Space and its Application to the 2008 Iwate-Miyagi Nairiku Earthquake," Geophys. J. Int., **184**, pp. 301–324.

[21] Kame, N., Saito, S., and Oguni, K., 2008, "Quasi-Static Analysis of Strike Fault Growth in Layered Media," Geophys. J. Int., **173**, pp. 309–314.

[22] Mikumo, T. and Miyatake, T., 1993, "Dynamic Rupture Processes on a Dipping Fault, and Estimates of Stress Drop and Strength Excess from the Results of Waveform Inversion," Geophys. J. Int., **112**, pp. 481–496.

[23] Bonnet, M., 1995, *Boundary Integral Equation Methods for Solids and Fluids*, John Wiley & Sons Ltd, Chichester.

[24] Aki, K. and Richards, P., 2002, *Quantitative Seismology*, 2nd ed., University Science Books, Sausalito.

[25] Tse, S. T. and Rice, J. R., 1986, "Crustal Earthquake Instability in Relation to the Depth Variation of Frictional Slip Properties," J. Geophys. Res., **91**, pp. 9452–9472.

[26] Burridge, R., 1969, "The Numerical Solution of Certain Integral Equations with Non-integrable Kernels Arising in the Theory of Crack Propagation and Elastic Wave Diffraction," Phil. Trans. R. Soc. London, Ser. A, **265**, pp. 353–381.